Anomalous anisotropy of fission fragments in near- and sub-barrier complete fusion-fission reactions of $^{16}O+^{232}Th$, $^{19}F+^{232}Th$, and $^{16}O+^{238}U$

Huanqiao Zhang, Zuhua Liu, Jincheng Xu, Xing Qian, Yu Qiao, Chengjian Lin, and Kan Xu
China Institute of Atomic Energy, Beijing, 102413, China
(Received 26 August 1993)

Using the fragment folding angle technique, the complete fusion-fission is separated from the transfer-induced fission. The cross sections of the complete fusion-fission and fragment angular distributions for the systems of $^{16}O+^{232}Th$, $^{19}F+^{232}Th$, and $^{16}O+^{238}U$ at near- and sub-barrier energies have been measured. The observed fission excitation functions can be fitted very well by coupled-channels theory calculations. It is found that fragments from complete fusion fission show a smaller angular anisotropy as compared with our previous measurements in which the transfer-induced fission component was not excluded. However, the measured angular anisotropies of complete fusion fission are obviously greater than expected on the basis of theoretical models in which the effect of prefission neutron emission was taken into account. Also the peak in the variation of the anisotropy with incident energy still persists in the $^{19}F+^{232}Th$ case.

PACS number(s): 25.70.Jj, 24.10.Eq

I. INTRODUCTION

Recently, anomalous anisotropies in the angular distributions of fission fragments resulting from heavy-ion induced fusion-fission reaction at near- and sub-barrier energies have been reported. They indicate that the fragment anisotropies are obviously greater than the theoretical model prediction [1,2] and a peak in the variation of the angular anisotropies with the incident energy exists in some systems [2,3]. These observations put forward an intriguing puzzle. On one hand, the models [4,5] which explicitly take into account the coupling of the relative motion coordinate in the entrance channel to other degrees of freedom can reproduce satisfactorily the fusion-fission excitation functions and explain the enhanced fusion cross sections at near- and sub-barrier energies rather well. On the other hand, under the assumption of all observed fission fragments resulting from compound nucleus decay, the theoretical predictions based on the saddle-point transition-state model (SPTS) with the transmission coefficient values, T_l, extracted from the above excitation function calculations fail to account for the experimental fission fragment angular distributions.

In addition, it is well established that, for the fissionable nucleus formed, the mean-square angular momentum value $\langle L^2 \rangle$ can be extracted from the anisotropy of fission-fragment angular distribution. The discrepancy described above implies that, although the theoretical fission cross sections show very good agreement with experiment, the models dramatically fail to predict the large mean-square angular momentum values which have been deduced from the measured fragment anisotropies. In contrast with the fusion-fission reactions, as pointed out by DiGregorio and Stokstad [6] based on a systematic analysis, the theoretical average angular momenta are in good agreement with the experimental data obtained from isomer ratio measurements and γ-ray multiplicities for almost all of the fusion-evaporation systems. Due to the reasons mentioned above, heavy-ion induced fusion fission at near- and sub-barrier energies has attracted much attention nowadays.

One thing should be stressed here. In the comparison between model calculation and measurement, it was assumed, on one hand, that the compound nucleus is formed by complete fusion and the compound nucleus undergoes fission after equilibrium. On the other hand, until recently the previous experiments were inclusive measurements, in which it could not be very sure that all fission fragments came from complete fusion fission (CFF). Some published experiments show that for heavier target nuclei discussed here noncompound fission, mainly transfer-induced fission (TF) has comparable contribution in the near- and sub-barrier energy region.

Very recently, there are a few experiments studying the transfer-induced fission. Lestone *et al.* [7] have measured the TF fragment angular distributions for the $^{16}O+^{232}Th$ system at energies of 86 MeV and 90 MeV. They found that the angular distributions integrated over all recoil angles, for the transfer-induced fission relative to the beam direction, have anisotropy values of 1.3 and 1.2 for 86 MeV and 90 MeV, respectively. The anisotropies are less pronounced than that observed when both CFF and TF components are mixed in the measurements. Thus, elimination of the TF contribution should result in about 5% increase of anisotropy for CFF alone at 86 MeV. Whereas Back *et al.* [8] have come to an opposite conclusion. At the same energy as Lestone, i.e., 86 MeV, they found that the CFF anisotropy value might have to decrease about 10% as compared with the result of the single measurement in which the TF component has not been excluded.

In order to have a sound basis for the comparison and to elucidate the mechanism of the discrepancy, it is necessary to separate in experiments the transfer-induced fission and to obtain data for complete fusion fission. Therefore, we started our experiments.

In the present experiment we have succeeded in separating the two components of CFF and TF in terms of the folding angle technique, and measured the complete fusion-fission cross sections and fragment angular distributions for the systems of $^{16}O+^{232}Th$, $^{19}F+^{232}Th$, and $^{16}O+^{238}U$ at near- and sub-barrier energies. The experimental complete fusion-fission excitation functions can be reproduced very well by the coupled-channels theory calculations. It is found that fragments from CFF show a smaller angular anisotropy as compared with earlier measurements in which the TF component was not excluded. The observed angular anisotropies of CFF fragments are obviously larger than the expectations of the saddle-point transition-state model, in which the influence of prefission neutron emission is taken into account. Also a peak in the variation of angular anisotropies with incident energy still persists in some cases.

II. EXPERIMENTAL PROCEDURE

The experiments were carried out with collimated ^{16}O and ^{19}F beams from the HI-13 tandem accelerator at the China Institute of Atomic Energy, Beijing. The targets of ^{232}Th and ^{238}U were about 350 $\mu g/cm^2$ thick. A Si(Au) detector was placed at $-20°$ relative to the beam direction as a monitor to detect the elastic scattering. Fission fragments were detected by two X-Y position sensitive double grid avalanche counters (DGAC), each with an active area of 20×25 cm^2, placed at either side of the beam. The distances from the centers of these counters to the target were 15 cm (forward counter) and 16 cm (backward counter) with corresponding angle coverages of $10° \leq \theta_{lab} \leq 90°$ and $-75° \leq \theta_{lab} \leq -160°$, respectively. These counters measured the position and the arrival time of the detected particles. The fission events were picked out by the coincidence measurement of two fragments. In off-line treatment, the fission events were taken from the central area (4 cm high $\times 25$ cm wide) of the DGAC counter. For every fission event, the coordinates of the points where the fragments hit each counter were transformed to the corresponding azimuthal angle ϕ_L and polar angle θ_L, taken with respect to the beam direction. Therefore, the folding angle θ_{FF} for every fission event was obtained. Displayed in Fig. 1 are the folding angle distributions for the $^{16}O+^{232}Th$ system at the laboratory energies of 78 MeV (left panel) and 86 MeV (right panel) with different angle ranges of emerging fragments, θ_{lab}, in the forward counter. Due to the difference of linear momentum transfer between fusion and transfer reactions, the distributions of the folding angle exhibit two peaks as shown in the figure. The left peak in the distributions is due to the transfer-induced fission events, while the right one is the peak of complete fusion fission. The solid lines in Fig. 1 are the Gaussian fit of the experimental data. The inverse open triangle points (TF) and open triangles (CFF) are the results of Monte Carlo simulation [9]. It can be seen from Fig. 1 that even at the most forward angle range (10°–20°) measured, the TF peak and CFF peak are still separated. The results of Monte Carlo simulation give a

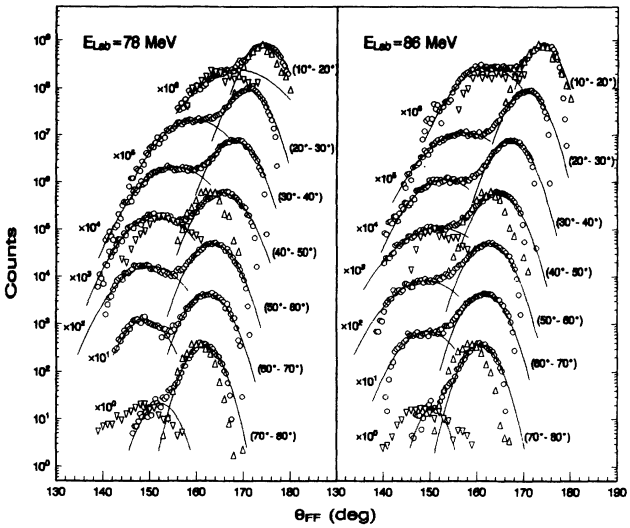

FIG. 1. The fragment folding angle distributions for the $^{16}O+^{232}Th$ fusion-fission reaction. The open circles are experimental data. The inverse open triangle points (TF) and open triangle points (CFF) are the results of Monte Carlo simulation.

reliable support for the above statement. It should be noted that in the 70°–80° angle range measured, the TF events were not completely detected due to the detection geometry. The present experiment could not provide the exact transfer-fission angular distribution. Anyhow, using the two distinguishable peaks in the fragment folding angle distribution, we have discriminated against possible contributions from TF component. As shown in Fig. 1, there is an overlap between the TF peak and the CFF peak. The area of this overlap increases as the laboratory angle θ_{lab} decreases. In the process of data analyses we have taken into account the overlap correction which is very small near $\theta_{lab} = 90°$ and about -10% at $\theta_{lab} = 10°$ for the component of complete fusion fission. The component arising from compound nucleus fission alone has been obtained successfully. The situations for the folding angle distributions for the systems of $^{19}F+^{232}Th$ and $^{16}O+^{238}U$ are similar to $^{16}O+^{232}Th$.

III. EXPERIMENTAL RESULTS

In present experiment we have obtained the fragment angular distributions of complete fusion fission for the systems of $^{16}O+^{232}Th$, $^{19}F+^{232}Th$, and $^{16}O+^{238}U$ at near- and sub-barrier energies. The total complete fusion-fission cross section was obtained by integration of the Legendre polynomial fit to the CFF angular distribution and normalizing to the cross section for Rutherford scattering. The experimental errors include the counting statistics, uncertainty of the overlap correction, and error of the extrapolation of angular distribution, etc. The total uncertainties for the fragment angular distribution data range between 4% and 8%, while for the fission cross sections, between 7% and 14%.

A. Fission excitation function

The excitation functions for the complete fusion-fission reactions of $^{16}O+^{232}Th$, $^{19}F+^{232}Th$, and $^{16}O+^{238}U$ are shown in Fig. 2. The solid lines in the figure were obtained by means of the coupled-channels theory with CCDEF code [10] in which the effects of the target static deformations were taken into account. In this code a nuclear potential $V_N(r,\theta)$ of the Christensen-Winther shape was used with $V_0 = -31R_PR_T/(R_P + R_T)$ MeV, $a_0 = 0.63$ fm, $R = R_P + R_T(\theta) + 0.29$ fm $+\Delta R$. The radius of the target $R_T(\theta)$ depends on the orientation of the symmetric axis of the target nucleus with respect to the colliding direction, and reads as

$$R_T(\theta) = R_T\left(1 + \sqrt{\frac{5}{4\pi}}\beta_2 P_2(\cos\theta) + \sqrt{\frac{9}{4\pi}}\beta_4 P_4(\cos\theta)\right). \quad (1)$$

Here $R_i = 1.233A_i^{1/3} - 0.98A_i^{-1/3}$, for $i = P,T$. The subscripts P,T stand for the projectile and target nuclei, respectively. The target nuclei have deformations $\beta_2 = 0.217$, $\beta_4 = 0.119$ for ^{232}Th and $\beta_2 = 0.224$, $\beta_4 = 0.050$ for ^{238}U. In these coupled-channels calculations, the following inelastic channels were included: excitation to the 0.7744 MeV state of ^{232}Th with $\beta_3 = 0.0932$, 0.7319 MeV state of ^{238}U with $\beta_3 = 0.084$ as well as the 0.1976 MeV state of projectile ^{19}F with $\beta_2 = 0.55$. It is seen from Fig. 2 that the agreement between the experimental and theoretical excitation functions are quite satisfactory for all the three systems. For each bombarding energy, the transmission coefficients T_l were obtained from these theoretical calculations.

B. Anisotropies of the fragment angular distributions

The anisotropy of fragment angular distribution $W(\theta)$ is defined as $A = W(0°)/W(90°)$. The measured fragment angular distributions for the complete fusion fission were extrapolated in terms of the Legendre polynomial with even terms, and the corresponding anisotropies were obtained with the extrapolation error of 4% or so. The variation of fragment anisotropies with the center-of-mass energy is presented in Figs. 3, 4, and 5 for the $^{16}O+^{232}Th$, $^{19}F+^{232}Th$, and $^{16}O+^{238}U$ reaction systems. The solid points and open circles in the figures are our CFF results and our previous inclusive data [2,3,11], respectively. In Fig. 3 the reversed triangles are the inclusive data of Vandenbosch *et al.* [1], solid and open triangles are the results of Back *et al.* [8,12] with and without the TF component eliminated. It can be seen that, for the complete fusion fission, our data are coincident with the results of Back *et al.* [8]. The open triangles and open squares in Fig. 4 are the experimental data of Fujiwara *et al.* [13] and Saxena *et al.* [14] for the $^{19}F+^{232}Th$ system, respectively. The observed anisotropies from our previous inclusive experiment are significantly greater than those of Fujiwara and Saxena. The reason of the discrepancy is not clear yet. It was claimed by Fujiwara that they had measured the TF angular distribution at $E_{c.m.} = 85.8$ MeV, and found the contribution of transfer-induced fission never enhances the anisotropy in inclusive measurements [15]. However, our data clearly show a peak in variation of fragment anisotropies with bombarding energy in $^{19}F+^{232}Th$ case. It is found, based on the comparison of the solid points with open circles in Figs. 3, 4, and 5, that the component arising from complete fusion fission alone shows a smaller angular anisotropy as compared with the results for TF and CFF components mixed. The theoretical fission fragment angular distributions were calculated in terms of the SPTS model with the effective moment of inertia J_{eff} derived from the rotating finite-range model (RFRM) [16] and the transition coefficients T_l extracted

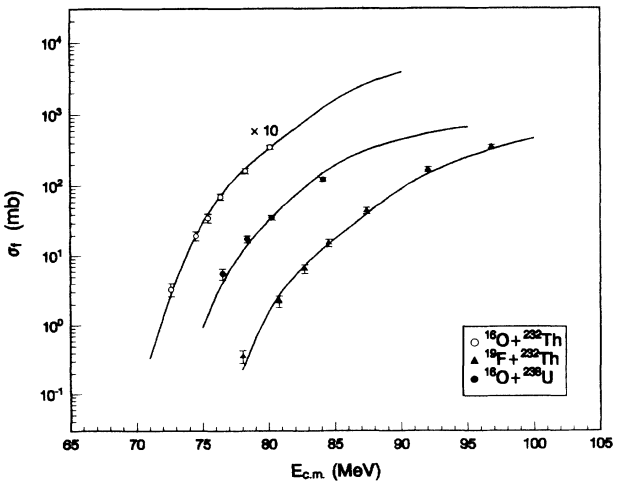

FIG. 2. Fission excitation functions. The solid curves are the calculations with the CCDEF code.

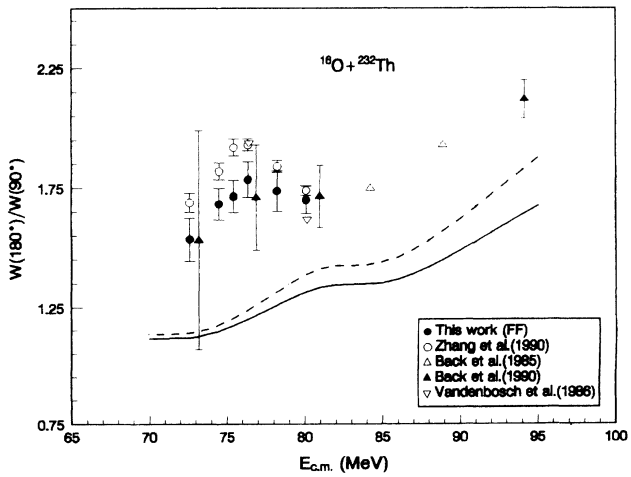

FIG. 3. Fission-fragment anisotropies as a function of bombarding energy for the $^{16}O+^{232}Th$ CFF reaction. The dashed and solid curves are the theoretical calculations of SPTS theory with and without the correction of prefission neutron emission.

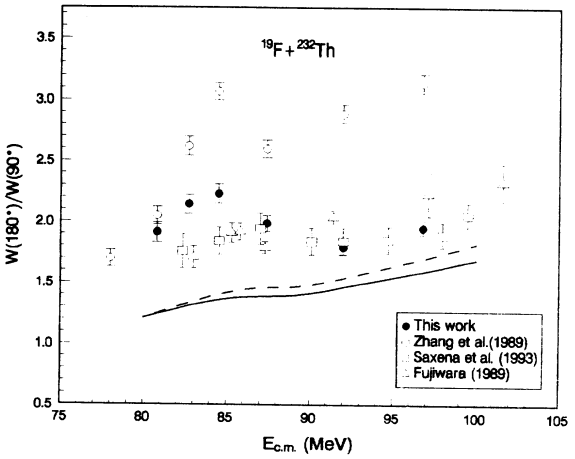

FIG. 4. Fission-fragment anisotropies as a function of bombarding energy for the $^{19}F+^{232}Th$ CFF reaction. The dashed and solid curves are the theoretical calculations of SPTS theory with and without the correction of prefission neutron emission.

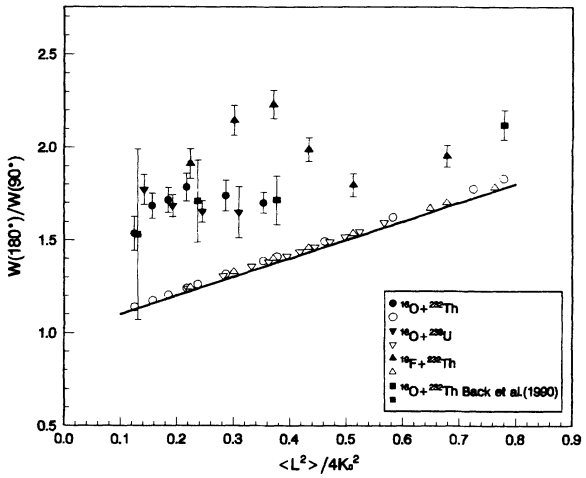

FIG. 6. CCF fragment anisotropies as a function of $\langle L^2\rangle/4K_0^2$. The solid and open symbols are the experimental data and theoretical calculation values, respectively. The solid squares are the data of Back *et al.*, the others are results of the present experiment. The solid line is from Eq. (2).

from the coupled-channels theory which reproduces the fission excitation function. The dashed and solid curves in Figs. 3, 4, and 5 are the theoretical predictions of the SPTS model with and without the correction of prefission neutron emission [17,18,14]. In the calculations, the experimental data of $\bar{\nu}_{\rm pre}$ [19] was used to determine the nuclear temperature at the saddle point. A few data in low excitation energies were obtained from the extrapolation with linear relation. This effect of prefission neutron emission is to increase the fragment anisotropy. The dashed curves represent the up limit of this correction.

In order to illustrate systematically the discrepancy between the observations and predictions, the fragment anisotropies of the complete fusion fission for all the three systems studied as a function of $\langle L^2\rangle/4K_0^2$ are shown in Fig. 6. Here the mean-square angular momenta, $\langle L^2\rangle$, are

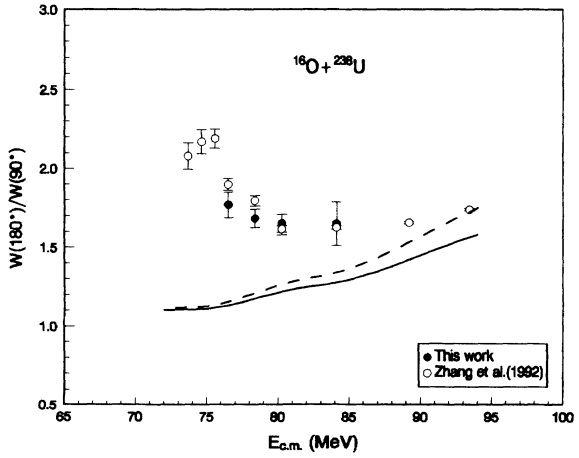

FIG. 5. Fission-fragment anisotropies as a function of bombarding energy for the $^{16}O+^{238}U$ CFF reaction. The dashed and solid curves are the theoretical calculations of SPTS theory with and without the correction of prefission neutron emission.

obtained from the calculations of the coupled-channels theory. $K_0^2 = J_{\rm eff}T/\hbar^2$ is the variance of the K distribution, i.e., the distribution of the projection of the compound nucleus spin J on the nuclear symmetric axis at saddle point. The effective moment of inertia, $J_{\rm eff}$ equals $J_{\|}J_{\perp}/(J_{\perp}-J_{\|})$. $J_{\|}$ and $J_{\perp}$ are the moments of inertia rotating around the symmetric axis and perpendicular axis, respectively. They were derived from the RFRM model as mentioned above. T is the nuclear temperature at saddle point. The anisotropy of the fission fragment angular distribution could be characterized by the approximate relation

$$A \approx 1 + \langle L^2\rangle/4K_0^2 \qquad (2)$$

shown as a straight line in Fig. 6. The solid and open symbols in the figure are the experimental data and theoretical predictions, respectively. The solid squares in Fig. 6 are the data of Back *et al.*, the other solid symbols are the results of the present work. It is obvious from the figure that the anisotropies are larger than expected theoretically.

C. The mean-square angular momentum $\langle L^2\rangle$

Equation (2) shows that the fragment anisotropy A determines the ratio $\langle L^2\rangle/4K_0^2$. If the K_0^2 values are known, then the mean-square angular momentum $\langle L^2\rangle$ of compound nucleus could be inferred from the measured fragment anisotropy. In the present work, the K_0^2 values were taken from the rotating finite-range model [16]. Displayed in Fig. 7 is the comparison of the observed mean-square angular momentum $\langle L^2\rangle_{\rm exp}$ for the complete fusion fission with the theoretical expectation as a function of the ratio of the center-of-mass energy to barrier height V_B. It is clearly shown that the experimental mean-square angular momentum values deduced

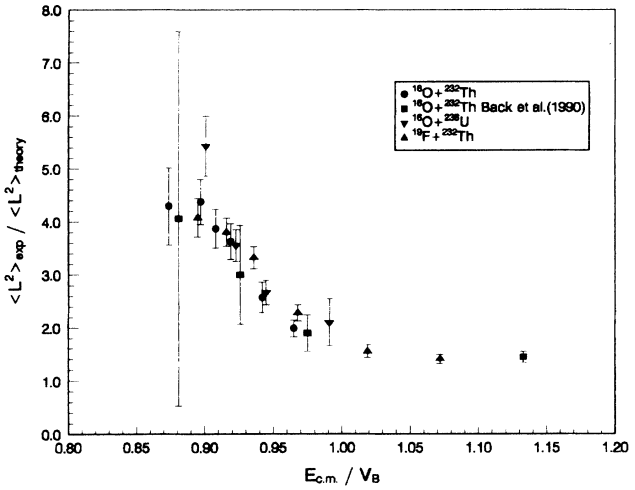

FIG. 7. Comparison of ratio of experimental to theoretical mean-square angular momentum values as a function of ratio of bombarding energy to barrier energy.

from the fission anisotropies are obviously greater than the predictions of the coupled-channels theory, although this model has reproduced the fission excitation functions satisfactorily.

IV. SUMMARY AND DISCUSSION

In the present work we have successfully separated the complete fusion fission and transfer-induced fission components in terms of the fragment folding angle technique, and measured the complete fusion fission cross sections and fragment angular distributions for the reaction systems of $^{16}O+^{232}Th$, $^{19}F+^{232}Th$, and $^{16}O+^{238}U$ at near- and sub-barrier energies. The experimental fission excitation functions are in quite good agreement with the predictions of the coupled-channels theory. It is found that the fragments arising from the complete fusion fission alone show a smaller angular anisotropy as compared with previous inclusive measurements in which the TF component was not excluded. However, the anisotropies found in the present experiment are, even with the prefission neutron emission correction, still obviously greater than expected on the basis of the saddle-point transition-state model with the transmission coefficients T_l extracted from the calculations of the coupled-channels theory. It may be seen from Figs. 3 and 4 that the anisotropies as a function of the center-of-mass energy persist to show a peak although not as pronounced as our previous inclusive results. The mean-square angular momenta $\langle L^2 \rangle_{\rm exp}$ were deduced from the fragment anisotropies in terms of relationship (2). The observed $\langle L^2 \rangle_{\rm exp}$ values are much greater than expected. It is obvious that the present standard models are inadequate for explaining both the fusion excitation function and the angular distributions of fission fragments simultaneously. In conclusion, the fragment anisotropies of the complete fusion fission are still anomalous, especially the peak exists, and the possibility that the observed anomalous anisotropies originate from transfer-induced fission can be ruled out. The challenge for a theoretical treatment of the sub-barrier fusion process is to describe simultaneously fusion excitation function and fission angular distributions. It is quite puzzling what is responsible for the observed anomaly in the complete fusion fission at near- and sub-barrier energies. This great difficulty makes us feel that we are still missing a major component of physics in the heavy-ion induced fusion-fission processes. Therefore, it appears to us that further research work is needed in order to get an understanding of the underlying physics.

ACKNOWLEDGMENTS

We would like to thank the operating staff of the tandem accelerator at CIAE for providing good conditions. This work was supported by the National Natural Science Foundation of China under Contract No. 19275067.

[1] R. Vandenbosch, T. Murakami, C.-C. Shahm, D. D. Leach, A. Rag, and M. J. Murphy, Phys. Rev. Lett. **56**, 1234 (1986); T. Murakami, C.-C. Shahm, R. Vandenbosch, D. D. Leach, A. Ray, and M. J. Murphy, Phys. Rev. C **34**, 1353 (1986).

[2] H. Zhang, J. Xu, Z. Liu, J. Lu, K. Xu, and M. Ruan, Phys. Lett. B **218**, 133 (1989).

[3] H. Zhang, J. Xu, Z. Liu, M. Ruan, and K. Xu, Phys. Rev. C **42**, 1086 (1990).

[4] C. H. Dasso, S. Landowne, and A. Winther, Nucl. Phys. **A405**, 381 (1983); **A407**, 221 (1983).

[5] H. Esbensen and S. Landowne, Nucl. Phys. **A467**, 136 (1987).

[6] D. E. DiGregorio and R. G. Stokstad, Phys. Rev. C **43**, 265 (1991).

[7] J. P. Lestone, J. R. Leigh, J. O. Newton, and J. X. Wei, Nucl. Phys. **A509**, 178 (1990).

[8] B. B. Back, R. R. Betts, P. Fernandez, B. G. Glagole, T. Happ, D. Henderson, H. Ikezoe, and P. Bent, in Fission at Sub-barrier Energies, presented at the Sixth Winter Workshop on Nuclear Dynamics, Jackson Hole, Wyoming, February 17–24, 1990; and private communication.

[9] X. Qian, J. Xu, Z. Liu, H. Zhang, T. Jiang, and Y. Ye, High Energy Phys. Nucl. Phys. (to be published).

[10] J. Fernandez-Niello, C. H. Dasso, and S. Landowne, Comput. Phys. Commun. **54**, 409 (1989).

[11] H. Zhang, Z. Liu, J. Xu, M. Ruan, X. Qian, K. Xu, and J. Lu, High Energy Phys. Nucl. Phys. **16**, 826 (1992).

[12] B. B. Back, R. R. Betts, J. E. Gindler, B. D. Wilkins, S. Saini, M. B. Tsang, C. K. Gelbke, W. G. Lunch, M. A. McMahan, and P. A. Baisden, Phys. Rev. C **32**, 195 (1985).

[13] H. Fujiwara, S. C. Jeong, Y. H. Pu, T. Mizota, H. Kugoh, Y. Futami, Y. Nagashima, and S. M. Lee, Anisotropy of fission fragment angular distributions for $^{19}F+^{232}Th$ near the Coulomb barrier, Report No. UTTAC-57, 1990, p. 52 (unpublished).

[14] A. Saxena, S. Kailas, A. Karnik, and S. S. Kapoor, Phys. Rev. C **47**, 403 (1993).
[15] H. Fujiwara, Fission fragment angular distributions for $^{19}F+^{232}Th$ near the Coulomb barrier, thesis, September 1990 (unpublished).
[16] A. J. Sierk, Phys. Rev. C **33**, 2039 (1986).
[17] H. Zhang, Z. Liu, J. Xu, X. Qian, S. Chen, and L. Lu, Chin. Phys. Lett. **9**, 297 (1992).
[18] H. Rossner, D. J. Hinde, J. R. Leigh, J. P. Lestone, J. O. Newton, J. X. Wei, and S. Elfstom, Phys. Rev. C **45**, 719 (1992).
[19] D. J. Hinde, H. Ogata, M. Tanak, T. Shimoda, N. Takashi, A. Shinohara, S. Wakamatsu, K. Katori, and H. Okamura, Phys. Rev. C **39**, 2268 (1989).